JACS
JOURNAL OF THE AMERICAN CHEMICAL SOCIETY

Communication

pubs.acs.org/JACS

Redox Mediator Effect on Water Oxidation in a Ruthenium-Based Chromophore–Catalyst Assembly

Michael R. Norris, Javier J. Concepcion, Daniel P. Harrison, Robert A. Binstead, Dennis L. Ashford, Zhen Fang, Joseph L. Templeton, and Thomas J. Meyer*

Department of Chemistry, University of North Carolina, Chapel Hill, North Carolina 27599-3290, United States

Supporting Information

ABSTRACT: The synthesis, characterization, and redox properties are described for a new ruthenium-based chromophore–catalyst assembly, $[(bpy)_2Ru(4\text{-Mebpy-}4'\text{-bimpy})Ru(tpy)(OH_2)]^{4+}$ (**1**, $[Ru_a^{II}\text{-}Ru_b^{II}\text{-}OH_2]^{4+}$; bpy = 2,2′-bipyridine; 4-Mebpy-4′-bimpy = 4-(methylbipyridin-4′-yl)-*N*-benzimid-*N*′-pyridine; tpy = 2,2′:6′,2″-terpyridine), as its chloride salt. The assembly incorporates both a visible light absorber and a catalyst for water oxidation. With added ceric ammonium nitrate (Ce^{IV}, or CAN), both **1** and **2**, $[Ru(tpy)(Mebim\text{-}py)(OH_2)]^{2+}$ (Mebim-py = 2-pyridyl-*N*-methylbenzimidazole), catalyze water oxidation. Time-dependent UV/vis spectral monitoring following addition of 30 equiv of Ce^{IV} reveals that the rate of Ce^{IV} consumption is first order both in Ce^{IV} and in an oxidized form of the assembly. The rate-limiting step appears to arise from slow oxidation of this intermediate followed by rapid release of O_2. This is similar to isolated catalyst **2**, with redox potentials comparable to the $[\text{-}Ru_b\text{-}OH_2]^{2+}$ site in **1**, but **1** is more reactive than **2** by a factor of 8 due to a redox mediator effect.

Water oxidation is the "other" half-reaction in solar fuels production.[1−3] Examples of single-site Ru,[4,5] Co,[6] Ir,[7,8] Cu,[9] and Fe[10] molecular catalysts have been reported, but for solar fuels applications these catalysts need to be integrated into molecular assemblies or other structures where light absorption can be used to drive water oxidation. A few molecular chromophore–catalyst assemblies containing water oxidation catalysts have been reported.[11−14] We report here the synthesis of a chromophore–catalyst assembly (**1**) for water oxidation, the mechanistic details of the catalytic oxidation reaction, and an enhanced rate of catalytic oxidation arising from a redox mediator effect.

Previous studies have shown that in ceric ammonium nitrate (Ce^{IV}, or CAN) water oxidation catalyzed by the blue ruthenium dimer, *cis,cis*-$[(bpy)_2(H_2O)\text{-}Ru^{III}ORu^{III}(OH_2)\text{-}(bpy)_2]^{4+}$, rate enhancements of up to 5000 can be achieved with added electron-transfer mediators such as $Ru(bpy)_3^{2+}$ either surface-bound[15] or in solution.[16] The mediator effect arises from the low barrier for electron transfer for the mediator, with a self-exchange rate constant for the $Ru(bpy)_3^{3+/2+}$ couple near the diffusion-controlled limit, 1.1×10^8 M^{-1} s^{-1}, compared to 1.1×10^3 M^{-1} s^{-1} for the $Ce^{IV/III}$ couple.[16] Redox mediator effects are also known in biology, where redox units undergoing facile electron transfer, e.g., iron–sulfur proteins, are used to shuttle redox equivalents between redox substrates.[17,18]

In addition to their ability to facilitate rapid electron transfer, $Ru(bpy)_3^{2+}$ complexes also absorb visible light. Assembly **1** links the redox mediator effect and light absorption with a known Ru single-site water oxidation catalyst, $[Ru(tpy)(Mebim\text{-}py)(OH_2)]^{2+}$, **2**, through a methylene bridge (Figure 1). The catalyst was chosen on the basis of results of a previous kinetic/mechanistic analysis which showed that the slow step in the overall oxidation of water by Ce^{IV} catalyzed by **2** is oxidation of $[Ru^{IV}{=}O]^{2+}$ to $[Ru^{V}(O)]^{3+}$.[4]

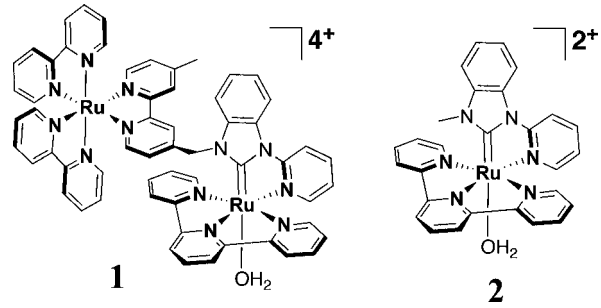

Figure 1. Chromophore–catalyst assembly **1** studied in this work and catalyst **2** that has been previously reported.

The synthesis of **1** (Figures S1–S3) was achieved in a stepwise manner by first preparing the bridging ligand. An N-alkylation reaction between 4-bromomethyl-4′-methyl-2,2′-bipyridine and 2-pyridyl-*N*-benzimidazole gave the bromide salt of the bridging ligand in good yield. The bipyridine functionality was then utilized in a selective reaction with $Ru(bpy)_2Cl_2$ to give $[Ru(bpy)_2(bpy\text{-}CH_2\text{-}bimpy)]^{3+}$. Subsequent reaction of this chromophore with the chloro-bridged ruthenium terpyridine dimer, $[Ru(tpy)Cl_2]_2$, in ethanol under microwave irradiation gave the desired dinuclear complex. After column chromatography on Sephadex LH-20 gel, a pure sample was obtained (^{1}H NMR, Figure S3).

As seen in the synthesis of **2**, only the isomer with the solvent molecule *trans* to the carbene[4] is evident in the ^{1}H NMR spectrum of **1**. The spectrum also displays diastereotopic protons for the methylene bridge as roofed doublets at 4.95 and 4.75 ppm (Figure S3). These protons appear as a singlet in the

Received: December 2, 2012
Published: January 21, 2013

   dx.doi.org/10.1021/ja311645d | *J. Am. Chem. Soc.* 2013, 135, 2080−2083

^{1}H NMR spectra of the free ligand and the chromophore (Figures S1 and S2).

Crystals of **1** were grown by slow diffusion of diethyl ether into an acetonitrile solution of **1**, giving the CH_3CN-coordinated assembly (Figure 2). Notably, the Ru2−C distance

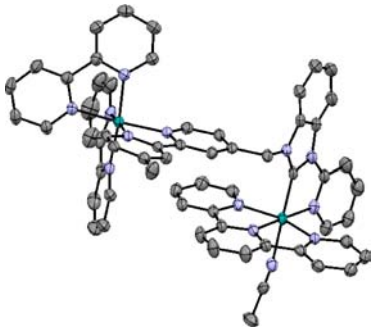

Figure 2. X-ray structure of the cation in *trans*-$[(bpy)_2Ru_a(4\text{-}Mebpy\text{-}4'\text{-}CH_2bimpy)Ru_b(tpy)(CH_3CN)](PF_6)_4$ (**1**$(PF_6)_4$) with thermal ellipsoids shown at the 50% probability level. Hydrogen atoms have been omitted for clarity.

(1.984 Å) in **1** is comparable to that found in **2** (1.943 Å), consistent with multiple Ru−C bonding.[19] The slight lengthening of the Ru−C bond by 0.041 Å in **1** relative to **2** is likely a result of the constrained geometry at **1** and the presence of the *trans* CH_3CN ligand in **1** relative to H_2O in **2**. In the crystal structure of **1**, the two Ru centers are located at a distance of 8.223 Å from each other. Because of the saturated link between metal centers, there is no orbital basis for extensive electronic interaction. The consequences of this are apparent in the additive nature of the UV/vis spectra of the constituents of **1**, $[Ru(bpy)_2(4,4'\text{-}Me_2bpy)]^{2+}$ (4,4′-Me_2bpy = 4,4′-dimethyl-2,2′-bipyridine) and $[Ru(tpy)(Mebim\text{-}py)(OH_2)]^{2+}$, relative to the spectrum of **1** as shown in Figure 3. Similar behavior was observed earlier in an amide-coupled assembly.[20]

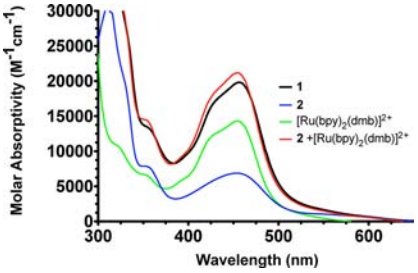

Figure 3. UV/vis spectra of **1** (black), **2** (blue), $[Ru(bpy)_2(4,4'\text{-}Me_2bpy)]^{2+}$ (green), and the addition of **2** and $[Ru(bpy)_2(4,4'\text{-}Me_2bpy)]^{2+}$ (red) in 0.1 M HNO_3.

Cyclic voltammetry (CV) measurements were carried out at a glassy carbon working electrode with a Ag/AgCl (3 M NaCl) reference (0.207 V vs NHE) and platinum counter electrode in buffered aqueous solutions with added 0.5 M KNO_3. A CV in 0.1 M HNO_3 shows the expected oxidations of the catalyst and chromophore parts of **1** (Figure 4). With scans to positive potentials, an initial reversible oxidation is observed at 0.91 V vs NHE for the $[Ru_a^{II}\text{-}Ru_b^{III}\text{-}OH_2]^{5+}/[Ru_a^{II}\text{-}Ru_b^{II}\text{-}OH_2]^{4+}$ couple, followed by a second reversible oxidation of the catalyst for the $[Ru_a^{II}\text{-}Ru_b^{IV}{=}O]^{4+}/[Ru_a^{II}\text{-}Ru_b^{III}\text{-}OH_2]^{5+}$ couple at 1.23 V. Both waves are pH dependent with the expected Nernstian behavior.

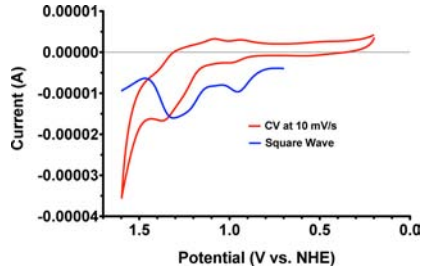

Figure 4. Cyclic voltammogram of **1** in 0.1 M HNO_3, 0.5 M in KNO_3 at 10 mV/s with a glassy carbon working electrode (0.07 cm^2, red) and a square wave voltammogram (blue) at 298 ± 3 K.

The $[Ru_a^{II}\text{-}Ru_b^{III}\text{-}OH_2]^{5+}/[Ru_a^{II}\text{-}Ru_b^{II}\text{-}OH_2]^{4+}$ couple is pH independent until the pK_a of $[Ru_a^{II}\text{-}Ru_b^{III}\text{-}OH_2]^{5+}$ is reached at pH 4.8. The potential for the $[Ru_a^{II}\text{-}Ru_b^{IV}{=}O]^{4+}/[Ru_a^{II}\text{-}Ru_b^{III}\text{-}OH_2]^{5+}$ couple decreases by 118 mV/pH unit with increasing pH, consistent with a $1e^-/2H^+$ couple. Past pH 4.8, the couples become $[Ru_a^{II}\text{-}Ru_b^{III}\text{-}OH]^{4+}/[Ru_a^{II}\text{-}Ru_b^{II}\text{-}OH_2]^{4+}$ and $[Ru_a^{II}\text{-}Ru_b^{IV}{=}O]^{4+}/[Ru_a^{II}\text{-}Ru_b^{III}\text{-}OH]^{4+}$, and $E_{1/2}$ values decrease with slopes of 59 mV/pH unit (Figure S4). Notably, $E_{1/2}$ values for these couples are only slightly less positive in **1**, by ∼0.08 V, than in **2**, and the two have comparable driving forces as oxidants. Beyond the $[Ru_a^{II}\text{-}Ru_b^{IV}{=}O]^{4+}/[Ru_a^{II}\text{-}Ru_b^{III}\text{-}OH_2]^{5+}$ and $[Ru_a^{II}\text{-}Ru_b^{III}\text{-}OH_2]^{5+}/[Ru_a^{II}\text{-}Ru_b^{II}\text{-}OH_2]^{4+}$ waves for the catalyst in **1**, a pH-independent wave appears at 1.31 V for oxidation of the chromophore, $[Ru_a^{III}\text{-}Ru_b^{IV}{=}O]^{5+}/[Ru_a^{II}\text{-}Ru_b^{IV}{=}O]^{4+}$. Significant water oxidation catalysis begins upon further oxidation of the catalyst to $[Ru_a^{III}\text{-}Ru_b^{V}(O)]^{6+}$, with the irreversible peak potential for the $[Ru_a^{III}\text{-}Ru_b^{V}(O)]^{6+}/[Ru_a^{III}\text{-}Ru_b^{IV}{=}O]^{5+}$ oxidation appearing at $E_{p,a} \approx 1.5$ V vs NHE.

With the addition of excess amounts of ceric ammonium nitrate (CAN), both **1** and **2** are catalysts for water oxidation, $2H_2O + 4Ce^{IV} \rightarrow O_2 + 4H^+ + 4Ce^{III}$. Time-dependent oxygen evolution measurements with Ce^{IV} added to **1** in 0.1 M HNO_3 were conducted by using a Foxy fluorescence probe, with evolved oxygen monitored in the headspace of the reaction vessel. The expected amount of oxygen, 7.5 equiv/30 equiv of Ce^{IV} added as CAN, was observed. Assembly **1** evolves oxygen in ∼100% yield based on added Ce^{IV} over a shorter time period than catalyst **2** (Figure 5). The enhanced rate of oxygen evolution with assembly **1** provides evidence for a redox mediator effect.

Hand-mixing experiments in a 2 mm flow cell were monitored by UV/vis kinetics measurements. Addition of a 30-fold excess of Ce^{IV} in 0.1 M HNO_3 to a 6.25×10^{-5} M

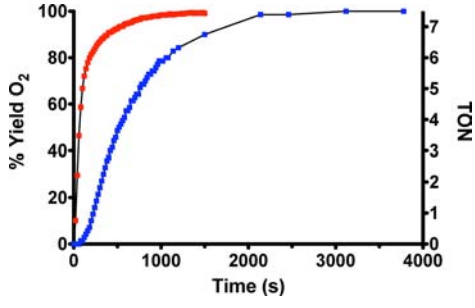

Figure 5. Oxygen appearance traces as measured with a Foxy fluorescence probe in the headspace over 10 mL solutions of 0.1 mM in **1** (red) or **2** (blue) in 0.1 M HNO_3 with 30 equiv of added CAN at 298 ± 3 K.

dx.doi.org/10.1021/ja311645d | J. Am. Chem. Soc. 2013, 135, 2080−2083

solution of **1** in 0.1 M HNO_3 results in rapid oxidation of **1**, as evidenced by loss of the visible Ru(II) MLCT absorptions for $[Ru_a^{II}\text{-}Ru_b^{II}\text{-}OH_2]^{4+}$. The UV/vis spectrum at the catalytic steady state is shown in Figure S5. For comparison with **2**, the kinetics of Ce^{IV} consumption by **1** were monitored in an identical fashion by observing the spectral change at 347 nm on the shoulder of the absorption maximum at λ_{max} = 318 nm for Ce^{IV} (ε = 3070 M^{-1} cm^{-1}). At this wavelength any absorbance change due to catalyst or chromophore is minimal and primarily reflects consumption of Ce^{IV}.

In the kinetic studies, the concentration of **1** was varied from 1.25×10^{-5} to 6.25×10^{-5} M and Ce^{IV} from 1.88×10^{-4} to 3.75×10^{-4} M. Under catalytic conditions with a large excess of Ce^{IV}, loss of Ce^{IV} (monitored at 347 nm) has an observed rate constant first order in $[Ce^{IV}]$ and first order in [**1**] (Figures S6 and S7). Similar kinetics were observed for **2**.[4] These observations are consistent with the rate law, $-d[Ce^{IV}] = k_{ox,1}[Ce^{IV}][\mathbf{1}_{ox}]$, with $[\mathbf{1}_{ox}]$ the concentration of a dominant, oxidized form of **1** at the catalytic steady state. From the data in Figures S6 and S7, $k_{ox,\mathbf{1}}$ = 272 M^{-1} s^{-1} for **1** in 0.1 M HNO_3 at 298 K. This rate constant is ~8 times larger than the rate constant for **2**, with $k_{ox,\mathbf{2}}$ = 33 M^{-1} s^{-1} under identical conditions.

Additional mixing experiments were carried out with **1** at 6.5×10^{-5} M with 1, 2, 3, 4, and 10 equiv of added Ce^{IV}. Addition of 3−4 equiv of Ce^{IV} resulted in complete loss of the $[Ru_a^{II}\text{-}Ru_b^{II}\text{-}OH_2]^{4+}$ metal-to-ligand charge-transfer absorptions. Global analysis of spectral changes following rapid hand-mixing with application of the spectral deconvolution program SPECFIT/32[21] provided spectral evidence for at least eight colored species (Figure S8) over the complete time course of the reaction beginning with $[Ru_a^{II}\text{-}Ru_b^{II}\text{-}OH_2]^{4+}$. The composition of the mixture of species changes dynamically during the course of the catalysis, with closely balanced overall rates for Ce^{IV} consumption and oxygen evolution at the catalytic steady state.

With excess (30 equiv) added Ce^{IV}, at the catalytic steady state, the visible absorption spectrum (Figure S5) is characterized by (i) loss of Ru^{II} MLCT features; (ii) appearance of a band at 655 nm consistent with $[Ru_a^{III}\text{-}Ru_b^{III}\text{-}OH_2]^{6+}$ that decays by pseudo-zero-order kinetics over a period of 400 s (Figure S9), and (iii) a near-IR band that absorbs at >900 nm and decreases by zero-order kinetics in 150 s (Figure S10). At the end of the catalytic cycle, with Ce^{IV} depleted, a final oxidized intermediate remains that returns the catalyst to $[Ru_a^{II}\text{-}Ru_b^{II}\text{-}OH_2]^{4+}$ (85−95%) with k = 0.012 s^{-1} (Figure S11).

A mechanism for water oxidation by single-site Ru catalysts such as $[Ru(tpy)(bpm)(OH_2)]^{2+}$ (tpy = 2,2′:6′,2″-terpyridine; bpm = 2,2′-bipyrimidine) and $[Ru(tpy)(bpy)(OH_2)]^{2+}$ has been established, based on the results of electrochemical and mixing studies with UV/vis monitoring with added Ce^{IV}.[4,22] A modified version is proposed for **1** in Scheme 1. This mechanism features (i) oxidative activation of the catalyst by stepwise proton-coupled electron-transfer oxidation from $[Ru^{II}\text{-}OH_2]^{2+}$ to $[Ru^{IV}{=}O]^{2+}$, (ii) further oxidation to $[Ru^{V}(O)]^{3+}$, (iii) O---O bond formation by atom-proton transfer[19,23] to give the peroxide intermediate $[Ru^{III}\text{-}OOH]^{2+}$, (iv) further oxidation to $[Ru^{IV}(OO)]^{2+}$ followed by slow O_2 loss and re-entry into the catalytic cycle as $[Ru^{II}\text{-}OH_2]^{2+}$, and/or (v) further oxidation to $[Ru^{V}(OO)]^{3+}$ followed by rapid loss of O_2 and re-entry into the catalytic cycle as $[Ru^{III}\text{-}OH]^{2+}$.

The mixing experiments with Ce^{IV} reveal that rapid oxidation of $[Ru_a^{II}\text{-}Ru_b^{II}\text{-}OH_2]^{4+}$ occurs to give a higher oxidation state form or forms that dominate at the catalytic steady state. Based on the cycle in Scheme 1, the higher oxidation state could be $[Ru_a^{III}\text{-}Ru_b^{IV}{=}O]^{5+}$, $[Ru_a^{III}\text{-}Ru_b^{V}(O)]^{6+}$, $[Ru_a^{III}\text{-}Ru_b^{III}\text{-}OOH]^{5+}$, or $[Ru_a^{III}\text{-}Ru_b^{IV}(OO)]^{5+}$, or a distribution of oxidation states. The first-order dependence of Ce^{IV} loss on $[Ce^{IV}]$ points to rate-limiting Ce^{IV} oxidation of $[Ru_a^{III}\text{-}Ru_b^{IV}{=}O]^{5+}$ to $[Ru_a^{III}\text{-}Ru_b^{V}(O)]^{6+}$, eq 1, or Ce^{IV} oxidation of $[Ru_a^{III}\text{-}Ru_b^{IV}(OO)]^{5+}$ to $[Ru_a^{III}\text{-}Ru_b^{V}(OO)]^{6+}$, eq 2. Both may play a role. $E_{1/2}$ values are ~1.5 V vs NHE for the $Ru^{V/IV}$ couples for both the oxo and peroxo couples, and, as noted above, there is evidence for two oxidized forms at the catalytic steady state. A similar ambiguity exists for Ce^{IV}-catalyzed water oxidation by **2**.[19]

Scheme 1. Proposed Mechanism[24]

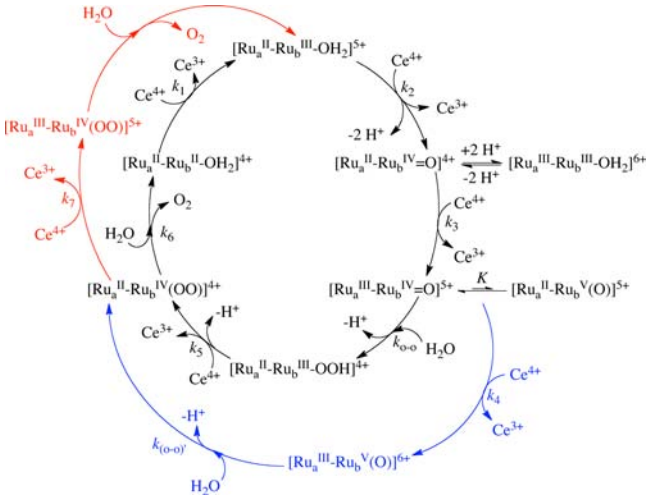

Based on the SPECFIT analysis, at the end of the catalytic cycle and after complete consumption of Ce^{IV}, the dominant product (85−95%) is $[Ru_a^{II}\text{-}Ru_b^{II}\text{-}OH_2]^{4+}$ (λ_{max} = 458 nm), which is formed with k = 0.012 s^{-1} (Figures S11 and S12). This observation is consistent with a catalytic cycle dominated by the "inner" catalytic loop in Scheme 1. The final step is loss of O_2 from $[Ru_a^{II}\text{-}Ru_b^{IV}(OO)]^{4+}$ with aquation to give $[Ru_a^{II}\text{-}Ru_b^{II}\text{-}OH_2]^{4+}$, k_6, with a lesser role for the red "outer" loop which results in $[Ru_a^{II}\text{-}Ru_b^{III}\text{-}OH_2]^{4+}$, k_7. The dominant pathway through k_6 may be a result of the labilizing effect of the carbene ligand *trans* to the O_2 binding site in the peroxide intermediate $[Ru_a^{II}\text{-}Ru_b^{IV}(OO)]^{5+}$. There is evidence for the buildup of peroxo intermediates for catalysts such as $[Ru(tpy)(bpm)\text{-}(OH_2)]^{2+}$ and $[Ru(tpy)(bpy)(OH_2)]^{2+}$ and for surface-bound analogues,[19,22,25,26] but there is no evidence for buildup of a peroxo intermediate for **2**.

Ce^{IV}-catalyzed water oxidation by **1** is more rapid than that by **2** by a factor of ~8, even though the energetics for the two oxidants are comparable. The enhanced rate constant provides evidence for a mediator effect by the chromophore in **1**. Based on the analysis above, $\Delta G^{\circ\prime} \approx -0.1$ eV for rate-limiting Ce^{IV} oxidation of $[Ru_a^{III}\text{-}Ru_b^{IV}{=}O]^{5+}$ to $[Ru_a^{III}\text{-}Ru_b^{V}(O)]^{6+}$, with $E^{\circ\prime}$ = 1.61 V for the $Ce^{IV/III}$ couple.

The origin of the mediator effect for the assembly may lie in the mechanism in Scheme 2 and pre-equilibrium formation of the high-energy "redox isomer", $[Ru_a^{II}\text{-}Ru_b^{V}(O)]^{5+}$, followed by "trapping" through oxidation via Ce^{IV} to $[Ru_a^{III}\text{-}Ru_b^{V}(O)]^{6+}$

dx.doi.org/10.1021/ja311645d | J. Am. Chem. Soc. 2013, 135, 2080−2083

Scheme 2. The Redox Mediator Effect

$$[Ru_a^{III}\text{-}Ru_b^{IV}{=}O]^{5+} \rightleftharpoons [Ru_a^{II}\text{-}Ru_b^{V}(O)]^{5+} : K$$

$$Ce^{IV} + [Ru_a^{II}\text{-}Ru_b^{V}(O)]^{5+} \rightarrow Ce^{III} + [Ru_a^{III}\text{-}Ru_b^{V}(O)]^{6+} : k_4$$

$$[Ru_a^{III}\text{-}Ru_b^{V}(O)]^{6+} + 2H_2O + Ce^{IV} \rightarrow [Ru_a^{III}\text{-}Ru_b^{II}\text{-}OH_2]^{4+} + Ce^{III} + O_2 + 2H^+ : \text{rapid}$$

(blue pathway). This mechanism is operable under excess Ce^{IV}. In this indirect mechanism, advantage is taken of the facile electron-transfer properties of the mediator. It avoids slow electron-transfer activation by direct Ce^{IV} oxidation of $[Ru_a^{III}\text{-}Ru_b^{IV}{=}O]^{5+}$ to $[Ru_a^{III}\text{-}Ru_b^{V}(O)]^{6+}$. From $E^{\circ\prime}$ values of ~1.5 V for the $[Ru_a^{III}\text{-}Ru_b^{V}(O)]^{6+}/[Ru_a^{III}\text{-}Ru_b^{IV}{=}O]^{5+}$ couple and $E^{\circ\prime}$ = 1.3 V for the $Ru_a^{3+/2+}$ couple as measured experimentally, $K = e^{-(\Delta G^{\circ\prime}/RT)} \approx 4 \times 10^{-4}$ for the equilibrium, $[Ru_a^{III}\text{-}Ru_b^{IV}{=}O]^{5+} \rightleftarrows [Ru_a^{II}\text{-}Ru_b^{V}(O)]^{5+}$. Based the mechanism proposed in Scheme 2 and the experimentally observed rate constant, $k_{obs,1} = k_4K = 272\ M^{-1}\ s^{-1}$. With $K = 4 \times 10^{-4}$ calculated from the aforementioned redox potentials of the relevant species, $k_4 = 7 \times 10^5\ s^{-1}$ for Ce^{IV} oxidation of $[Ru_a^{II}\text{-}Ru_b^{V}(O)]^{5+}$ to $[Ru_a^{III}\text{-}Ru_b^{V}(O)]^{6+}$, a reaction favored by −0.3 eV. Note that Scheme 2 refers to the mechanism in 0.1 M HNO_3, consistent with all mixing experiments.

Our results are important in identifying a redox mediator effect in a chromophore−catalyst assembly that combines light absorption and water oxidation catalysis, in our case using Ce^{IV} as the oxidant. Redox mediation is a phenomenon tied to the redox potentials of the assembly and the relatively slow electron-transfer characteristics of the oxidant. The mechanistic analysis presented here should be general for related chromophore−catalyst assemblies, including recent examples based on use of persulfate anion, $S_2O_8^{2-}$, as an oxidative quencher for initiating water oxidation.[27,28]

■ ASSOCIATED CONTENT

Ⓢ Supporting Information

Crystallographic data; experimental details, including ^1H NMR spectra, oxygen measurements, and electrochemical and kinetic analysis. This material is available free of charge via the Internet at http://pubs.acs.org.

■ AUTHOR INFORMATION

Corresponding Author

tjmeyer@unc.edu

Notes

The authors declare no competing financial interest.

■ ACKNOWLEDGMENTS

This work was wholly funded by the UNC Energy Frontier Research Center (EFRC) "Center for Solar Fuels", an EFRC funded by the U.S. Department of Energy, Office of Science, Office of Basic Energy Sciences, under Award DE-SC0001011, supporting M.R.N, D.L.A., D.P.H., J.J.C., R.A.B., and Z.F. We acknowledge support for the purchase of instrumentation from the UNC EFRC (Center for Solar Fuels, an EFRC funded by the U.S. Department of Energy, Office of Science, Office of Basic Energy Sciences, under Award DE-SC0001011) and UNC SERC ("Solar Energy Research Center Instrumentation Facility" funded by the U.S. Department of Energy, Office of Energy and Efficiency & Renewable Energy, under Award DE-EE0003188).

■ REFERENCES

(1) Lewis, N. S.; Nocera, D. G. *Proc. Natl. Acad. Sci. U.S.A.* **2006**, *103*, 15729.

(2) Alstrum-Acevedo, J. H.; Brennaman, M. K.; Meyer, T. J. *Inorg. Chem.* **2005**, *44*, 6802.

(3) Concepcion, J. J.; Jurss, J. W.; Brennaman, M. K.; Hoertz, P. G.; Patrocinio, A. O. T.; Iha, N. Y. M.; Templeton, J. L.; Meyer, T. J. *Acc. Chem. Res.* **2009**, *42*, 1954.

(4) Concepcion, J. J.; Jurss, J. W.; Norris, M. R.; Chen, Z.; Templeton, J. L.; Meyer, T. J. *Inorg. Chem.* **2010**, *49*, 1277.

(5) Kaveevivitchai, N.; Zong, R.; Tseng, H.-W.; Chitta, R.; Thummel, R. P. *Inorg. Chem.* **2012**, *51*, 2930.

(6) Wasylenko, D. J.; Palmer, R. D.; Schott, E.; Berlinguette, C. P. *Chem. Commun.* **2012**, *48*, 2107.

(7) Blakemore, J. D.; Schley, N. D.; Balcells, D.; Hull, J. F.; Olack, G. W.; Incarvito, C. D.; Eisenstein, O.; Brudvig, G. W.; Crabtree, R. H. *J. Am. Chem. Soc.* **2010**, *132*, 16017.

(8) Parent, A. R.; Brewster, T. P.; De Wolf, W.; Crabtree, R. H.; Brudvig, G. W. *Inorg. Chem.* **2012**, *51*, 6147.

(9) Barnett, S. M.; Goldberg, K. I.; Mayer, J. M. *Nature Chem.* **2012**, *4*, 498.

(10) Fillol, J. L.; Codola, Z.; Garcia-Bosch, I.; Gomez, L.; Pla, J. J.; Costas, M. *Nature Chem.* **2011**, *3*, 807.

(11) Bignozzi, C. A.; Schoonover, J. R.; Scandola, F. *Inorg. Chem.* **1997**, *1997*, 1.

(12) Kaveevivitchai, N.; Chitta, R.; Zong, R.; El Ojaimi, M.; Thummel, R. P. *J. Am. Chem. Soc.* **2012**, *134*, 10721.

(13) Song, W.; Glasson, C. R. K.; Luo, H.; Hanson, K.; Brennaman, M. K.; Concepcion, J. J.; Meyer, T. J. *J. Phys. Chem. Lett.* **2011**, *2*, 1808.

(14) Li, F.; Jiang, Y.; Zhang, B.; Huang, F.; Gao, Y.; Sun, L. *Angew. Chem., Int. Ed.* **2012**, *51*, 2417.

(15) Jurss, J. W.; Concepcion, J. C.; Norris, M. R.; Templeton, J. L.; Meyer, T. J. *Inorg. Chem.* **2010**, *49*, 3980.

(16) Sigler, P. B.; Masters, B. J. *J. Am. Chem. Soc.* **1957**, *79*, 6353.

(17) Kroeger, A.; Innerhofer, A. *Eur. J. Biochem.* **1976**, *69*, 487.

(18) Dementin, S.; Burlat, B.; Fourmond, V.; Leroux, F.; Liebgott, P.-P.; Abou Hamdan, A.; Leger, C.; Rousset, M.; Guigliarelli, B.; Bertrand, P. *J. Am. Chem. Soc.* **2011**, *133*, 10211.

(19) Concepcion, J. J.; Tsai, M.-K.; Muckerman, J. T.; Meyer, T. J. *J. Am. Chem. Soc.* **2010**, *132*, 1545.

(20) Ashford, D. L.; Stewart, D. J.; Glasson, C. R.; Binstead, R. A.; Harrison, D. P.; Norris, M. R.; Concepcion, J. J.; Fang, Z.; Templeton, J. L.; Meyer, T. J. *Inorg. Chem.* **2012**, *51*, 6428.

(21) Spectrum Software Associates.

(22) Concepcion, J. J.; Jurss, J. W.; Templeton, J. L.; Meyer, T. J. *J. Am. Chem. Soc.* **2008**, *130*, 16462.

(23) Chen, Z.; Concepcion, J. J.; Hu, X.; Yang, W.; Hoertz, P. G.; Meyer, T. J. *Proc. Natl. Acad. Sci. U.S.A.* **2010**, *107*, 7225.

(24) Redox states for the peroxo intermediates are assigned on the basis of observations from $[Ru(tpy)(bpy)(OO)]^{n+}$ and $[Ru(tpy')(bpy)(OO)]^{n+}$, where redox couples for the peroxides are at lower potential than the aquo complexes, although they are not directly observed in this work.

(25) Chen, Z.; Concepcion, J. J.; Hull, J. F.; Hoertz, P. G.; Meyer, T. J. *Dalton Trans.* **2010**, *39*, 6950.

(26) Vannucci, A. K.; Hull, J. F.; Chen, Z.; Binstead, R. A.; Concepcion, J. J.; Meyer, T. J. *J. Am. Chem. Soc.* **2012**, *134*, 3972.

(27) Hara, M.; Waraksa, C. C.; Lean, J. T.; Lewis, B. A.; Mallouk, T. E. *J. Phys. Chem. A* **2000**, *104*, 5275.

(28) Morris, N. D.; Suzuki, M.; Mallouk, T. E. *J. Phys. Chem. A* **2004**, *108*, 9115.